On the (in)accuracy of the spherical particle approximation in mineral aerosol radiative forcing simulations

Michael Kahner[1], Timo Nousiainen[2], and Petri Räisänen[3]

[1]*Swedish Meteorological and Hydrological Institute, 601 76 Norrköping, Sweden*
[2]*University of Helsinki, Finland*
[3]*Finnish Meteorological Institute, Finland*

Abstract

Errors in mineral aerosol radiative forcing computations due to the spherical particle approximation (SPA) and the uncertainty in refractive index were studied. These two error sources are found to be of comparable magnitude, although strongly dependent on optical depth, surface albedo, and particle size. Thus, the use of the SPA in radiative transfer simulations may be among the major error sources in quantifying the regional climate forcing by mineral aerosols.

1 Introduction

Mineral aerosols are radiatively important owing to their widespread distribution and their relatively high optical depth [1]. Desertification caused by changes in land usage results in rising mineral dust concentrations, which is considered the dominant anthropogenic radiative forcing mechanism in and near arid regions [2]. Quantification of this radiative forcing effect is subject to various error sources, of which the uncertainty in the refractive index m and, to a lesser extent, the uncertainty in the size distribution (SD) have previously been identified as the most important ones [2]. It is common in climate applications to model optical properties of dust aerosols by use of spherical model particles. The validity of the spherical particle approximation (SPA) is rarely questioned in climate research, and it is often taken for granted that the errors caused by the SPA are small compared to those caused by other error sources. In the present study we put this assumption to a test.

2 Optical properties of mineral aerosols

Table 1 shows the aerosol samples employed in the simulations, their effective radii r_{eff}, and the uncertainty ranges of their refractive indices $m = n + i\kappa$. Also shown are the optical depths assumed in the radiative transfer simulations. The optical properties of these nonspherical dust particles are derived from measure-

Sample	r_{eff} (μm)	n	κ	τ
Feldspar	1.0	1.5–1.6	10^{-5}–10^{-3}	0.25
Red Clay	1.5	1.5–1.7	10^{-5}–10^{-3}	0.25
Green Clay	1.55	1.5–1.7	10^{-5}–10^{-3}	0.25
Loess	3.9	1.5–1.7	10^{-5}–10^{-3}	1.10
Sahara	8.2	1.5–1.7	10^{-5}–10^{-3}	1.10

Table 1: Mineral aerosol samples considered in this study.

ments available in the Amsterdam Light Scattering Database [3] (*http* : *//www.astro.uva.nl/scatter*), which

provides particle SDs and phase matrices at wavelengths of 441.6 nm and 632.8 nm for scattering angles of 5°–173°. The full phase function and the asymmetry parameter g are derived by combining the measured phase functions with Mie-computations of the diffraction peak through a variational data analysis method. The details of the procedure and a discussion of analysis errors can be found in Ref. [4].

To obtain corresponding results for spheres, and to estimate the m-uncertainty, we ran Mie simulations based on the measured SDs. The refractive index of each sample has been varied within the uncertainty ranges indicated in Tab. 1. The extreme values of g are obtained for $m_1 = n_{\min} + i\kappa_{\max}$ and $m_2 = n_{\max} + i\kappa_{\min}$. Figure 1 shows a comparison of asymmetry parameters derived from the measurements and the Mie computations. It is evident from the figure that the SPA-errors and m-related errors (estimated for spheres)

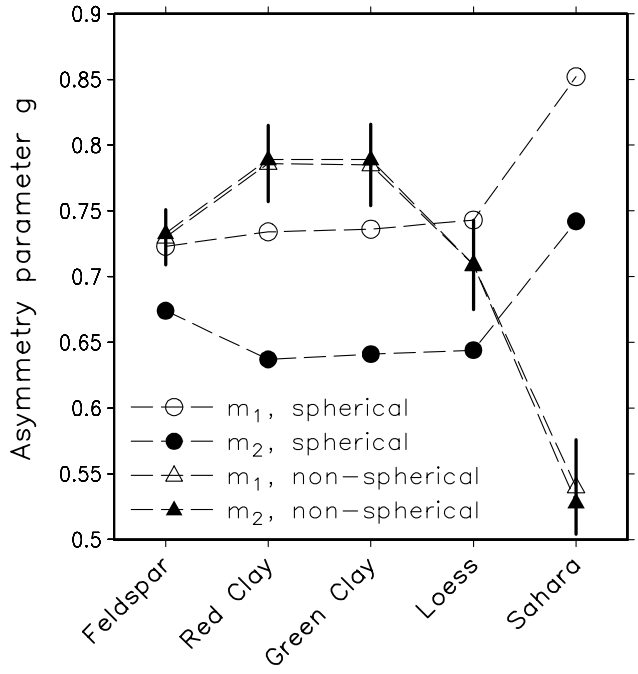

Figure 1: Values of the asymmetry parameter g at λ=441.6 nm for spherical and non-spherical aerosol particles and for refractive indices $m_1 = n_{\min} + i\kappa_{\max}$ and $m_2 = n_{\max} + i\kappa_{\min}$. The vertical bars indicate the uncertainty of g for non-spherical particles, defined as best estimate ± measurement error (one standard deviation). The m-dependence of g for non-spherical particles is artificially small since m affects only the diffraction part of the combined phase function.

in g are of comparable magnitude.

The single-scattering albedo is known to be rather insensitive to particle shape. Hence, values obtained from Mie calculations were used both for spherical and non-spherical particles.

3 Radiative transfer simulations

Radiative transfer simulations were performed for a standard tropical atmosphere. The aerosols are assumed to be spread uniformly between 0 and 5 km. The solar zenith angle is 55° (a yearly daytime-average at an altitude of 20°). Two surface albedos were used: $\alpha_s = 0.1$ (ocean surface) and $\alpha_s = 0.45$ (high-albedo desert). The lower optical depth ($\tau = 0.25$) indicated in Table 1 lies within the range of typical background values near arid regions, whereas the higher value ($\tau = 1.10$) is typical for dust-storm events.

4 Comparison of radiative flux and transmittance errors

We investigate the errors in the net radiative flux at the top of the atmosphere (TOA) (Fig. 2a), the flux absorbed within the atmosphere (Fig. 2b), the downwelling flux at the surface (BOA = bottom of atmosphere) (Fig. 2c), and the net flux at the surface (Fig. 2d). For instance, Fig. 2a shows three normalised net radiative flux errors at the TOA for a wavelength of λ=441.6 nm and for a surface albedo of α_s=0.1:

$$\delta F^{(\mathrm{net})}_{\mathrm{spher}}(m) = 100\% \times \left[F^{(\mathrm{net})}_{\mathrm{spher}}(m_1) - F^{(\mathrm{net})}_{\mathrm{spher}}(m_2)\right] / (2F_{\mathrm{solar}}) \quad (1)$$

$$\delta F^{(\mathrm{net})}_{\mathrm{m_1}}(\mathrm{SPA}) = 100\% \times \left[F^{(\mathrm{net})}_{\mathrm{spher}}(m_1) - F^{(\mathrm{net})}_{\mathrm{nonspher}}(m_1)\right] / F_{\mathrm{solar}} \quad (2)$$

$$\delta F^{(\mathrm{net})}_{\mathrm{m_2}}(\mathrm{SPA}) = 100\% \times \left[F^{(\mathrm{net})}_{\mathrm{spher}}(m_2) - F^{(\mathrm{net})}_{\mathrm{nonspher}}(m_2)\right] / F_{\mathrm{solar}}. \quad (3)$$

Here, $F^{(\mathrm{net})}_{\mathrm{nonspher}}$ and $F^{(\mathrm{net})}_{\mathrm{spher}}$ denote spectral net fluxes computed using optical properties for non-spherical and spherical aerosols, respectively. Hence, $\delta F^{(\mathrm{net})}_{\mathrm{spher}}(m)$ (black bars) is the normalised net flux error related to the uncertainty in m, based on computations for spherical particles. It is defined here by dividing the maximal m-related uncertainty range by a factor of two. Similarly, $\delta F^{(\mathrm{net})}_{\mathrm{m_1}}(\mathrm{SPA})$ (shaded bars) and $\delta F^{(\mathrm{net})}_{\mathrm{m_2}}(\mathrm{SPA})$ (white bars) represent the net radiative flux errors caused by the SPA for refractive indices m_1 and m_2, respectively. The normalised errors in atmospheric absorptance (Fig. 2b), downwelling flux at the surface (Fig. 2c) and net flux at the surface (Fig. 2d) are defined analogously. The main result in Fig. 2a is that the SPA-related errors in the TOA net flux $\delta F^{(\mathrm{net})}_{\mathrm{m_1}}(\mathrm{SPA})$ and $\delta F^{(\mathrm{net})}_{\mathrm{m_2}}(\mathrm{SPA})$ are in most cases comparable to, and sometimes even larger than the error related to the m-uncertainty $\delta F^{(\mathrm{net})}_{\mathrm{spher}}(m)$. Another result is that there are clear differences between $\delta F^{(\mathrm{net})}_{\mathrm{m_1}}(\mathrm{SPA})$ and $\delta F^{(\mathrm{net})}_{\mathrm{m_2}}(\mathrm{SPA})$. Thus the SPA and the uncertainty in the refractive index are strongly correlated error sources in net flux simulations.

Similar observations apply to the BOA transmitted and net fluxes in Figs. 2c and 2d. Thus the SPA- and m-related errors in these radiative quantities are of comparable size. On the other hand, the error in the absorbed flux (Fig. 2b) is entirely dominated by the uncertainty in m.

Computations for a surface albedo of $\alpha_s = 0.45$ indicated that for the TOA net flux, the m-related error is larger and the SPA-error is smaller than for $\alpha_s = 0.10$. The absorbed flux error is, as expected, again dominated by the m-error. At BOA, however, the SPA-error still dominates over the m-error in net-flux and transmitted-flux computations.

Finally, we remark that the flux errors considered here can equivalently be regarded as radiative forcing errors, since radiative forcing is defined as $\Delta F = F_{\text{aerosols included}} - F_{\text{no aerosols}}$, where the aerosol-free case is not impacted by the treatment of aerosol optical properties.

5 Conclusions

The primary conclusion of this study is that the use of spherical model particles (Mie theory) can introduce substantial errors in simulated mineral aerosol radiative forcing at the TOA and at the surface. The errors are comparable to those related to the uncertainty in the refractive index m, which is generally believed to be the largest error source. Due to the widespread use of the SPA in aerosol climate studies, this error source could have far-reaching consequences in assessing the direct climate forcing effect of mineral aerosols.

The SPA errors arise through the misrepresentation of the phase function and the related error in the asymmetry parameter g. Moreover, the radiative flux errors caused by the SPA appear rather unpredictable and defy simplistic corrections, since their magnitude and sign depend on particle size, surface albedo, wavelength, and optical depth, and since they are strongly correlated with the radiative flux errors caused by the m-uncertainty. The SPA-related TOA and surface net-flux errors are more pronounced over the ocean, whereas the significance of the corresponding m-related errors increase over land surfaces. The error in the downwelling flux at the surface is much less sensitive to surface albedo.

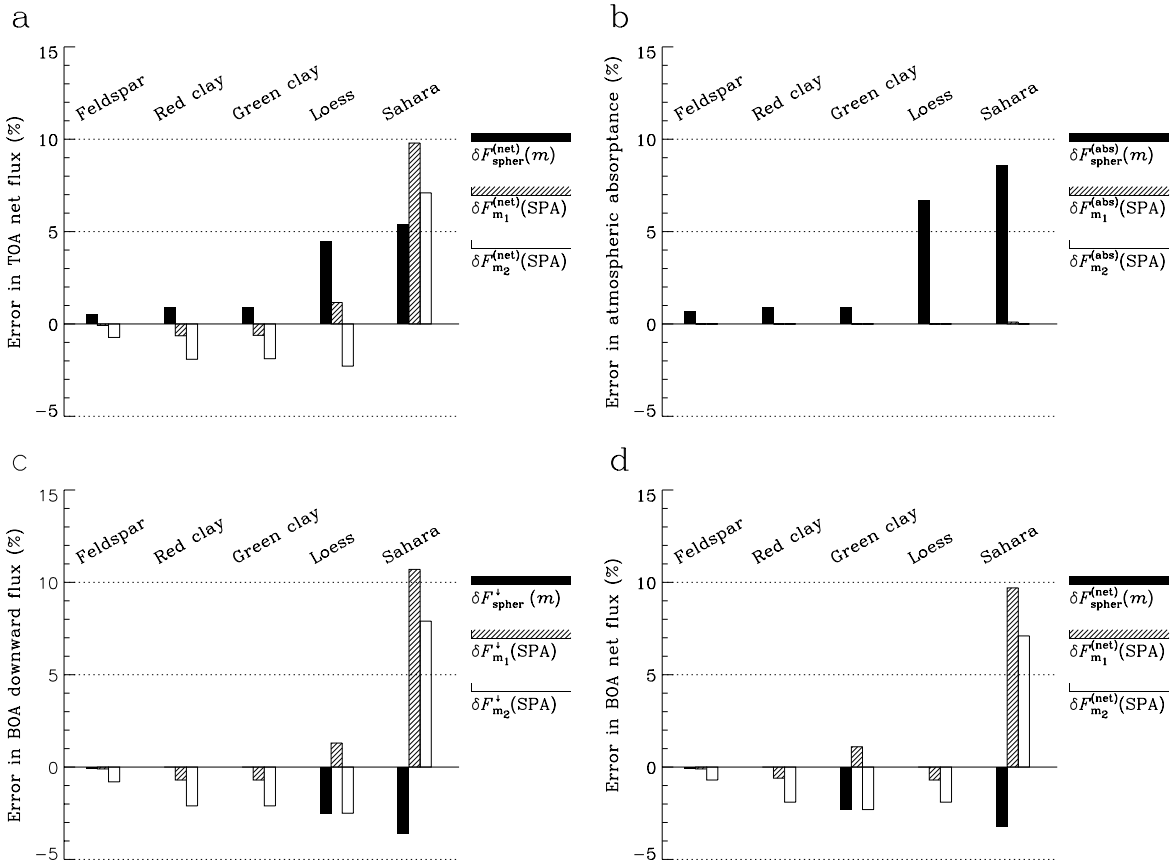

Figure 2: (a) Normalised spectral net flux errors at TOA (as defined by Eqs. (1)–(3)) for the five aerosol samples at a wavelength of 441.6 nm and a surface albedo of 0.1. (b)–(d) Same as (a), but for the errors in atmospheric absorptance, downward flux at the surface (BOA), and net flux at the surface, respectively.

References

[1] I. N. Sokolik, D. M. Winker, G. Bergametti, D. A. Gilette, G. Carmichael, Y. J. Kauman, L. Gomes, L. Schuetz, and J. E. Penner. Outstanding problems in quantifying the radiative impacts of mineral dust. *J. Geophys. Res.*, 106:18015–18027, 2001.

[2] G. Myhre and F. Stordal. Global sensitivity experiments of the radiative forcing due to mineral aerosols. *J. Geophys. Res.*, 106:18193–18204, 2001.

[3] H. Volten, O. Muñoz, E. Rol, J. F. de Haan, W. Vassen, J. W. Hovenier, K. Muinonen, and T. Nousiainen. Scattering matrices of mineral aerosol particles at 441.6 nm and 632.8 nm. *J. Geophys. Res.*, 106:17375–17401, 2001.

[4] M. Kahnert and T. Nousiainen. Variational data analysis method for combining laboratory-measured light scattering phase functions and forward-scattering computations. *J. Quant. Spectrosc. Radiat. Transfer*, 103:27–42, 2007.